SYNTHESIS OF SrTiO₃ NANOPOWDER BY SOL-GEL-HYDROTHEMAL METHOD FOR GAS SENSING APPLICATION

D. D. Kajale[1], G. E. Patil[1], V. B. Gaikwad[2], S. D. Shinde[2], D. N. Chavan[3], N. K. Pawar[4], S. R. Shirsath[1]

G. H. Jain[1*]

[1]Materials Research Lab., Arts, Commerce and Science College, Nandgaon 423 106, India.

[2]Materials Research Lab., K.T.H.M. College, Nashik 422 005, India.

[3]Department of Chemistry, Arts, Commerce and Science College, Lasalgaon 422 306, India.

[4]Department of Physics, Arts, Commerce and Science College, Satana 423 105, India.

Emails: gotanjain@rediffmail.com

Abstract- Strontium titanate (SrTiO₃) nanopowder has been synthesized through a sol-gel-hydrothermal method. The X-ray diffraction studies of SrTiO₃ nanopowder have shown that the as-prepared powder was single phase, crystalline, and has a cubic perovskite structure (ABO₃) with a lattice constant a = 3.903 Å. The particle size calculated from FWHM was ~22 nm. SrTiO₃ nanopowder was examined using thermo gravimetric analysis; differential thermal analysis and UV-visible absorption spectroscopy. The transmission electron microscopic investigations have shown that the particle size of the as-prepared powder has a mean size of 34 nm. Then highly sensitive and selective sensors to H₂S based on glass substrate were fabricated successfully by screen-printing

technique. Sensitivity, selectivity, response time, and recovery time of the sensors were systematically investigated as a function of operating temperature, using H_2S, CO, CO_2, H_2, Cl_2, LPG, C_2H_5OH, O_2, NH_3 and NO_2 as test gases. The sensitivity was found to lie below and around the ppm level for H_2S gas at 150^oC.

Index terms*: SrTiO_3, sol-gel-hydrothermal, nanocrystalline, thick film, gas response, H_2S gas sensor.

I.   INTRODUCTION

Nanostructured materials have been generating tremendous interests in the past years due to their fundamental significance for addressing some basic issues in fundamental physics, as well as their potential applications as advanced materials with collective properties [1]. Perovskite-type oxides are some of the most fascinating materials in condensed-matter research. Strontium titanate, $SrTiO_3$ (ST), is arguably the prototypical member of this structure family, not only because it can be made to exhibit a diverse range of unusual properties itself. Moreover, STO is an important n-type semiconductor with band gap of about 3.2 eV [2], and it has been widely studied not only because of its variety of outstanding physical properties (stability, wavelength response, and current–voltage) but also for its practical applications, such as their high static dielectric constant and good insulation [3,4], their use in grain boundary barrier-layer capacitors [5], resistive oxygen gas sensors [6,7], solar cells [8], solid oxide electronic device [9], at large scale, as substrate at the time of growth of thin films perovskite compounds [10], and promising candidate for efficient photocatalysts [11] and photoelectrodes [12,13].

It is well known that the properties of nanoparticles depend not only of the synthesis method and chemical composition but also on their structure, shape, and size [14-15]. Therefore, the ability to tune the size and shape of ST particles is significant for fundamental studies as well as for the preparation of ceramics and composite materials with tailored properties. There were many synthesis methods applied to prepare pure and doped ST, including solid-state reaction [16], sol-gel method [17, 18], micro-emulsion method [19], hydrothermal synthesis [20–23], and the polymeric precursor method [24–26]. Recently, controlled homogeneity of the precursor gel in the synthesis of ST nanoparticles by an epoxide- assisted sol-gel route was reported by Cui et al. [27].

Among these various synthetic methods, hydrothermal or chemical reaction methods are of great interest because they are safe and environmentally friendly synthesis performed at moderate temperatures (around $200^{o}C$) and they are effective methods for creating novel architectures or hierarchical structures based on nanocrystals. [28]

The development of gas sensors has received considerable attention in recent years, especially in the monitoring of environmental pollution. It is well known that performance of gas sensors are regulated by their sensitivity, selectivity, response/recovery speed, stability, and reproducibility [29–31].

The gas sensing is a surface phenomenon of gas-solid interaction, where the conductivity of semiconducting oxides can be altered by adsorption of gases from ambient. It is well known that depending upon the morphology and operating temperatures; the oxide surface hold various oxygen species, such as O^-, O^{2-}, and O_2^-. Their number and distribution also plays an important role in the gas sensing characteristics. The literature shows that the metal oxide nanoparticles enhance the sensitivity of a gas sensing material, while the selectivity is achieved by doping on surface or in the volume. However, recently Korotcenkov [32] suggested that the shape control of the nanocrystallites can provide energetically different adsorption sites for the test gases on different crystal facets. Thus existence of large surface to volume ratio in the typical nanostructured material facilitates better response towards specific gases. Moreover, morphology and particle size of nanomaterials depend upon their method of preparation and sintering temperatures, and hence one can observe different responses towards gases for the similar composition.

Hydrogen sulfide (H_2S) is a corrosive, colorless, toxic, and flammable gas, occurring naturally in crude petroleum, natural gas, volcanic gases, and hot springs with smell of rotten eggs. It can also be produced from industrial activities that include food processing, coking ovens, craft paper mills, tanneries, and petroleum refineries [33].

To date, various semiconductor gas sensors have been employed to detect trace concentrations of H_2S, including those that use SnO_2, CuO-doped SnO_2, and In_2O_3 [34-36]. It should be noted that the H_2S sensors found in the literature often show slow or irreversible recovery reactions. This hampers the application of H_2S sensors to commercial enterprises. From the viewpoint of applications, a small size and low power consumption are other important issues, which can be

best accomplished when the micromachining technology is applied to the fabrication of a micro-heater and microelectrodes.

In this work we report a route to directly synthesize cubic highly nanocrystalline $SrTiO_3$ powder using $TiCl_4$ and $SrCl_2$ as starting materials by the sol-gel hydrothermal method in an oxygen atmosphere. The electrical and gas-sensing properties of the films prepared are reported.

II.   EXPERIMENTAL

a. Preparation of nanocrystalline $SrTiO_3$

In a typical procedure, $TiCl_4$ was diluted with 2 M HCl to form a yellowish solution, and $Sr(OH)_2.8H_2O$ was dissolved in deionized water. The two solutions were mixed to form strontium titanium solution. With stirring and N_2 bubbling, 6 M NaOH was added to the strontium titanium solution, forming a white homogeneous colloidal strontium titanium slurry. The mixed solution was transferred into a 500 ml Teflon-lined stainless steel reactor, sealed, and then heated at 180 ^{o}C and kept for 12–48 h under an oxygen partial pressure of 60 psi. At the end of the reaction the autoclave was allowed to cool to room temperature. The as-synthesized white powder that attached to the bottom and inner wall of the Teflon container was collected, centrifuged, washed with distilled water and ethanol to remove the remaining ions, and dried at 60 ^{o}C for 6 h under reduced pressure.

b. Sensor Fabrication

The screen-printing technique was used to manufacture the sensors. In this process, a thixotopic paste of as-synthesized white powder is pressed through a screen on to the substrate using a rubber squeeze.The thixotropic paste of sensor material suitable for screen-printing was formulated by adding 75 wt% of the fine powder of ST to 25 wt% of the organic binder (solution of ethyl cellulose in a mixture of organic solvents such as butyl cellulose, butyl carbitol acetate and terpineol etc.) The binder was used to provide the necessary viscosity for the screen-printing process. After mixing the powder with the organic binder, the paste was milled in a planetary ball mill in order to homogenize the mixture. This thixotropic paste then used for screen-printing of thick films on glass substrate in the desired pattern [37, 38].

The thickness of films was measured by using weight difference method. The thicknesses of the films were observed in the range from 65-75 µm. The reproducibility in the thickness of the films

was possible by maintaining proper rheology and thixotropy of the paste. The films were dried at 80-100 ^{o}C for 0.5 h. Sintering of the dried films was carried out by heating at temperature 550 ^{o}C in the furnace for 30 min.

c. Characterization

The obtained powders were characterized by X-ray powder diffraction (XRD) (Bruker D8) with Cu-Kα radiation (λ = 1.5406 Å) in the 2θ range from 20° to 80° with 0.02^{o} min^{-1}. TG-DTA analyses were carried out with a Netzsch-409 STA apparatus with a heating rate of 20°C min^{-1} under flowing air. Microstructural characterization was performed by scanning electron microscopy (SEM, JEOL 2300) and transmission electron microscopy (Philips EM 200 make) with selected area electron diffraction (SAED). The samples for transmission electron microscope (TEM) were prepared by ultrasonically dispersing the powder in methanol and allowing a drop of this to dry on a carbon-coated copper grid. A UV–visible absorption measurement was performed to analyze the optical properties of the prepared sample. The dispersions of the nanoparticles were prepared in deionized water for the UV–visible absorption measurements.

III.   RESULT AND DISCUSSION

a. XRD analysis

The typical room temperature XRD pattern of the as-synthesized white powder is shown in Figure 1 All the peaks are indexed for cubic SrTiO$_3$ single phase material. The lattice constant calculated from the XRD data is 3.903Å that agrees with the reported XRD data in JCPDS file (JCPDS 35-0734) for SrTiO$_3$. No secondary phase was observed in the XRD patterns in the as-repared powder, thereby indicating that SrTiO$_3$ phase formation was complete during the process itself.   In contrast, all the previous wet chemical methods including combustion synthesis produced a single phase material only after calcination at temperature $\geq$1000 ^{o}C.
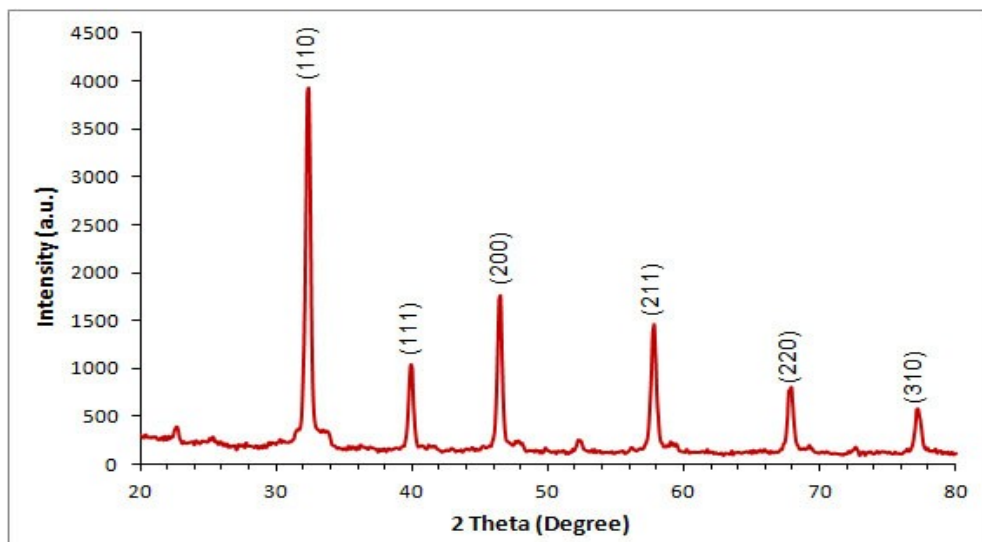
Figure 1. XRD patterns of as-prepared $SrTiO_3$ nanopowder.

b. Thermal analysis

The thermal characterization of the nanoparticles of $SrTiO_3$ synthesized through the sol-gel-hydrothermal process was carried out using differential thermal analysis and thermo gravimetric analysis up to 1200^oC at heating rate of $20^oC/min$ in nitrogen atmosphere. Figure 2 shows the DTA and TGA curves of the as-prepared powders of $SrTiO_3$. No notable changes were observed in the TGA as well as in DTA curves of the obtained product. The total weight loss for a temperature range of $30\text{-}1200^oC$ in the TGA curve is $< 3\%$ and this weight loss can be due to the adsorbed moisture present in the sample.
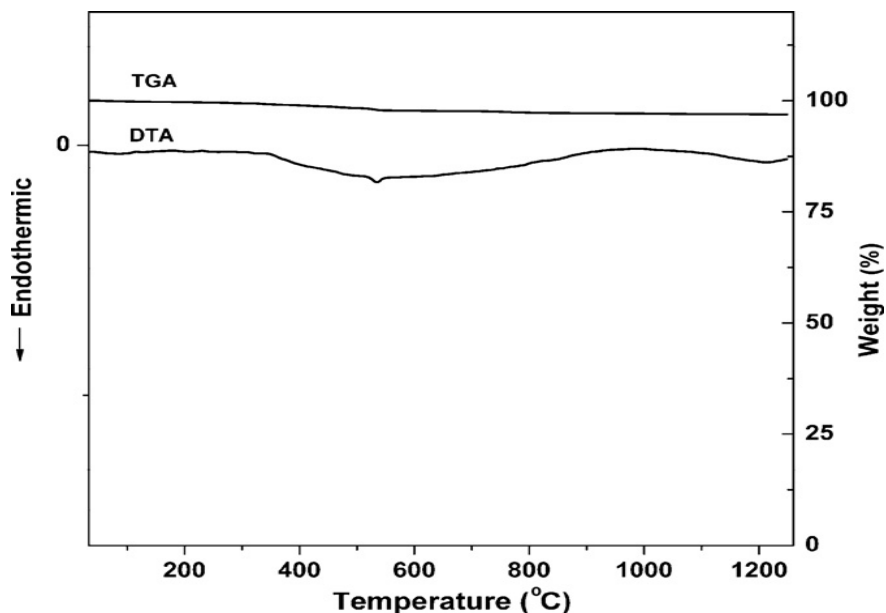

Figure 2. TGA–DTA curves of as-prepared $SrTiO_3$ nanopowder.

c. Microstructural analysis

Figure 3(a) and (b) show the TEM micrograph of the synthesized product and selected area electron diffraction (SAED) pattern. The particles were submicron-sized agglomerates consisting of nanocrystallites. The TEM showed well faceted particles with sharp boundaries, thereby indicating that no amorphous secondary phases are segregated at the grain boundaries. In agreement with the XRD results, all the rings in the SAED pattern were indexed for cubic perovskite structure. Table 1 compares the lattice spacing (d values) calculated from XRD and SAED patterns. A deviation of ~3% was observed in the d-values, which most likely arise from the difference in wavelengths of X-ray and electron beam used for recording the diffraction pattern. The average particle size calculated from a number of TEM images was 34 nm with a standard deviation of 14 nm. It is worth noting here that by using electrochemical impedance spectroscopy Balaya et al [39] showed that $SrTiO_3$ particles up to a mean diameter of ~80 nm behaves as electrically mesoscopic. $SrTiO_3$ particles synthesized in the present work also fall within this size regime.
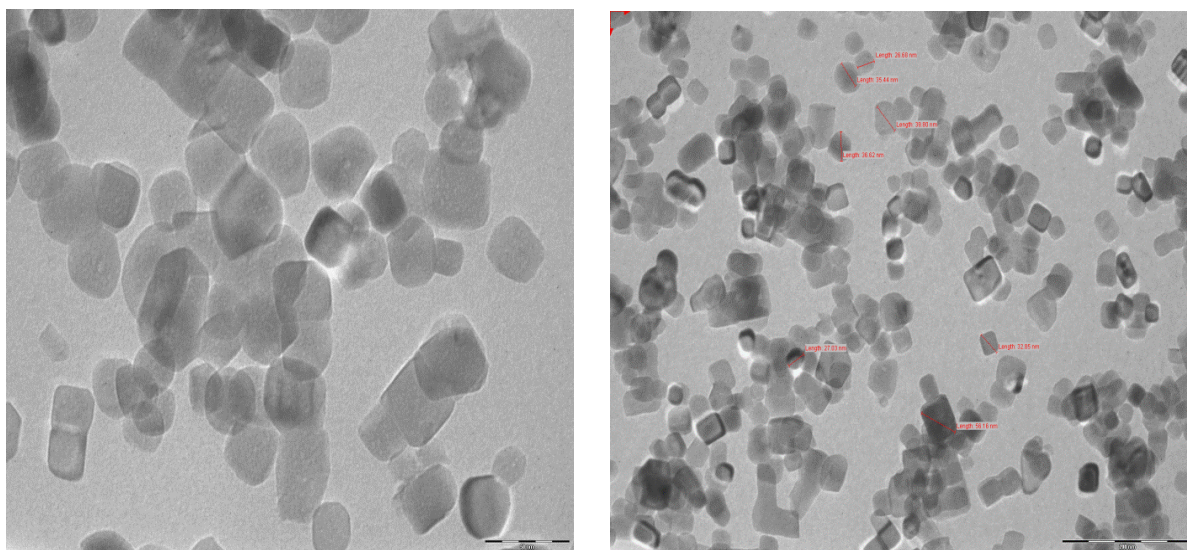
(a)
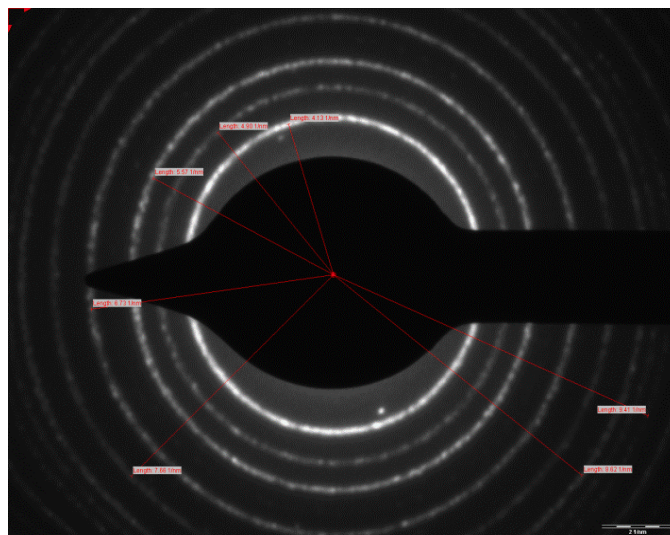
(b)

Figure 3. (a) TEM, and (b) SAED pattern of the SrTiO$_3$ nanopowder.

Table 1: Lattice spacing for different crystal planes as measured from XRD and SAED pattern

h k l	d$_{XRD}$ (Å)	d$_{ED}$(Å)
1 1 0	2.767	2.837
1 1 1	2.257	2.316
2 0 0	1.955	2.008
2 1 1	1.595	1.635
2 2 0	1.381	1.422
3 1 0	1.232	1.242

d. UV– visible absorption spectra of SrTiO$_3$

Figure 4 shows the UV–visible absorption spectrum of the as-prepared SrTiO$_3$ nanopowder. As can be seen, this product displays a wide absorption peak centered at around 343 nm (3.4 eV), which is slightly blue-shifted compared with the band gap of bulk SrTiO$_3$ [40]. Besides, there is an absorption tail at the lower energy side, which may be due to the presence of surface states and defect levels in the nanocrystalline product [41, 42]
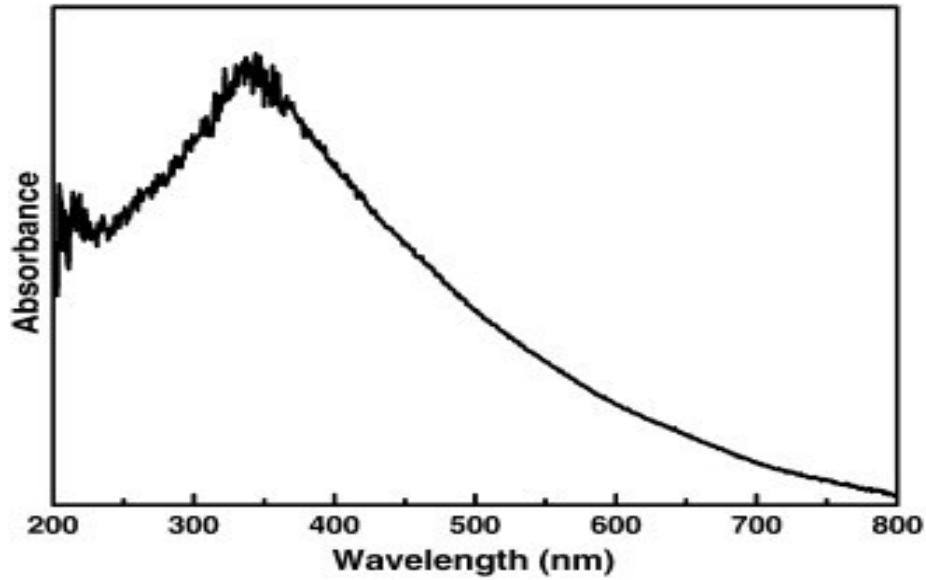
Figure 4. UV– vis absorption spectra of $SrTiO_3$.

e.   Electrical properties

i.   I–V Characteristics

Fig. 5 depicts the conductivity of pure ST at room temperature. The symmetrical nature of the I–V characteristics for particular samples shows that the contacts are Ohmic in nature
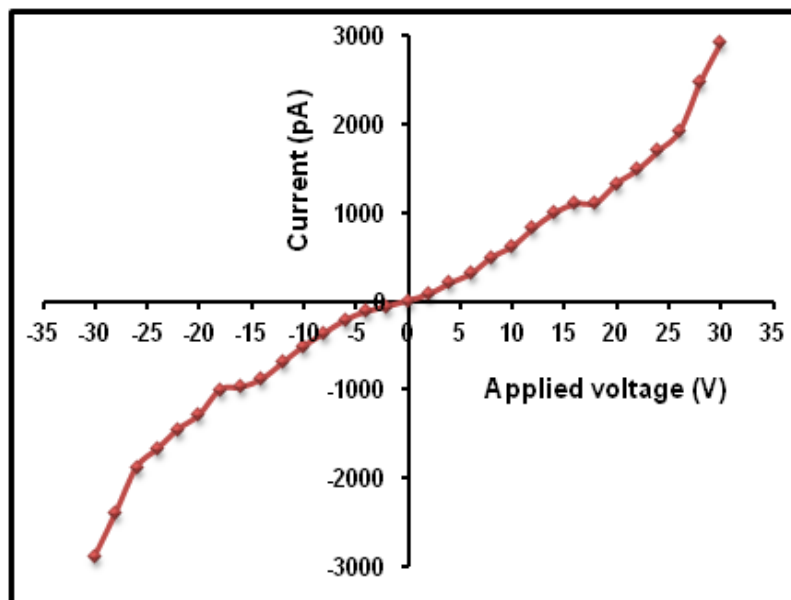

Figure 5. I–V characteristics plot of the Nano ST thick film.

ii. Electrical conductivity

The semiconducting nature of ST is observed from the measurements of conductivity with operating temperature. The semiconductivity in ST must be due to large oxygen deficiency in it. The material would then adsorb the oxygen species at higher temperatures $(O_2^- \rightarrow 2O^- \rightarrow O^{2-})$.

It is clear from Fig. 6 that the conductivity of pure ST film increase with an increase in operating temperature in ambient, indicating a negative temperature coefficient of resistance. This behavior confirmed the semiconducting nature of ST.
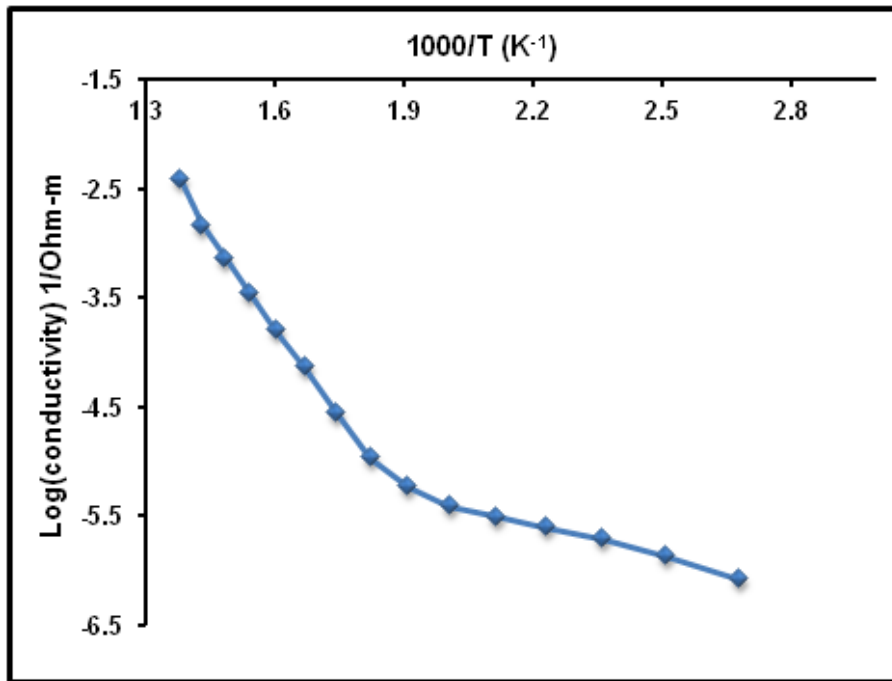

Figure 6. Variation of conductivity with operating temperature.

f. Gas sensing properties of ST thick films

i. Gas response with temperature

Gas response of a sensor was defined as the ratio of the change in conductance of a sample on exposure to the test gas to the conductance in air.

$$\text{Gas Response} = \frac{|Gg|}{|Ga|} = \frac{\Delta}{|Ga|} \qquad (1)$$

Where *Gg* & *Ga* are conductance of a sample in the presence and absence of a test gas respectively & ΔG is the change in conductance.

It has been firstly investigated that the optimal operating temperatures of the sensor, nano $SrTiO_3$ thick film, to different testing gases. Figure 7 shows the gas response plots of the $SrTiO_3$ sensor towards 80 ppm H_2S and 200 ppm of other different testing gases like C_2H_5OH, ammonia (NH_3), CO_2, CO, Cl_2, LPG, H_2, NO_2, O_2 at different operating temperature. The response of $SrTiO_3$ sensor towards H_2S increases rapidly and reaches its maximum at the operating temperature of 150 ^oC, and then decreases with further increasing the temperature. The same behavior is observed in the case of other testing gases, and their maximum responses appear at different temperature. Among the testing gases, the $SrTiO_3$ sensor shows the highest response towards H_2S. The magnitude of the response descends in the order of H_2S, C_2H_5OH, and NH_3, which seems to be correlated with the interaction strength between the testing gas and the sensing layer [43]. The response of the $SrTiO_3$ sensor to H_2S reaches the maximum value of 543 at 150 ^oC, which is about 5.43 and 20.74 times higher than the responses of C_2H_5OH, and NH_3 achieved at the 350 ^oC, respectively. This operating temperature of 150 ^oC could be useful for an improved selectivity of gas sensor to H_2S.
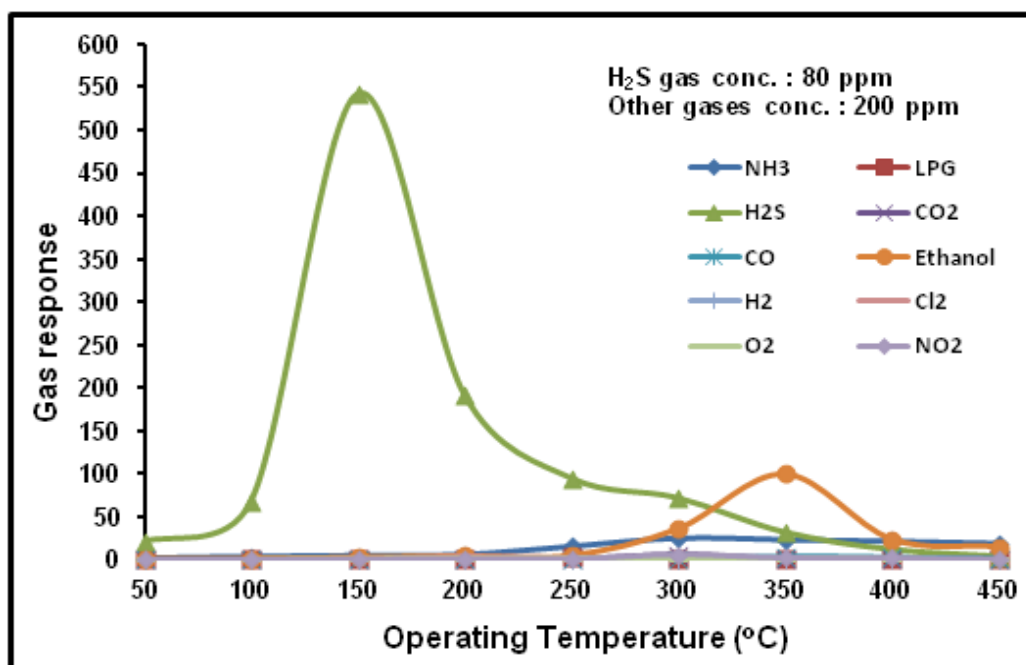

Figure 7. Variation of gas response of ST thick film with operating temperature.

ii.   *Selectivity of ST thick film*

The ability of a sensor to respond to a certain gas in presence of other gases is known as selectivity. A good sensor will discern a particular signal by allowing adsorption of the desired gas while remaining insensitive to others.
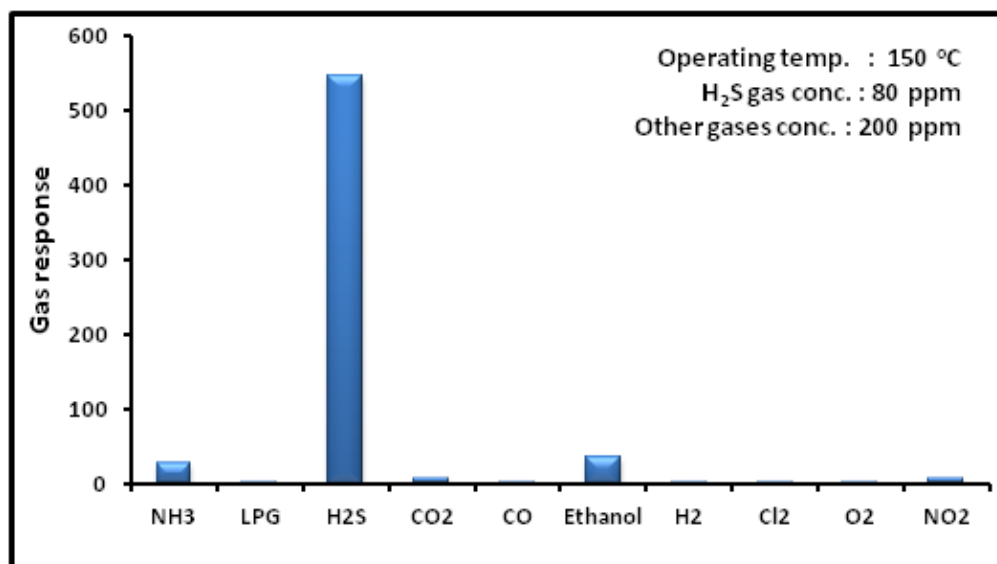

Figure 8. Selectivity of ST thick film.

Figure 8 depicts the selectivity of nano $SrTiO_3$ thick films to 80 ppm of H_2S gas against various gases (200 ppm) at 150 ^{o}C. It is clear from figure that, nano $SrTiO_3$ thick films shows not only enhanced response towards H_2S but also very high selectivity.

iii.   *Variation of gas response with H₂S gas concentration*

The dependence of gas response of ST thick films with the H_2S concentration at an operating temperature of 150°C is shown in Figure 9 It is observed that the Gas response increases linearly as the H_2S concentration increases from 10–80 ppm and then decreases with further increase in the H_2S concentration. The linear relationship between the Gas response and the H_2S concentration at low concentrations may be attributed to the availability of sufficient number of sensing sites on the film to act upon the H_2S. The low gas concentration implies a lower surface coverage of gas molecules, resulting into lower surface reaction between the surface adsorbed oxygen species and the gas molecules. The increase in the gas concentration increases the surface reaction due to a large surface coverage. Further increase in the surface reaction will be gradual when saturation of the surface coverage of gas molecules is reached. Thus, the maximum sensitivity was obtained at an operating temperature of 150°C for the exposure of 80 ppm of H_2S.

The $SrTiO_3$ is able to detect up to 10 ppm for H_2S with reasonable sensitivity at an operating temperature of 150 °C. The linearity of the sensitivity in the low H_2S concentration range (10–80 ppm) suggests that the $SrTiO_3$ can be reliably used to monitor the concentration of H_2S over this range.
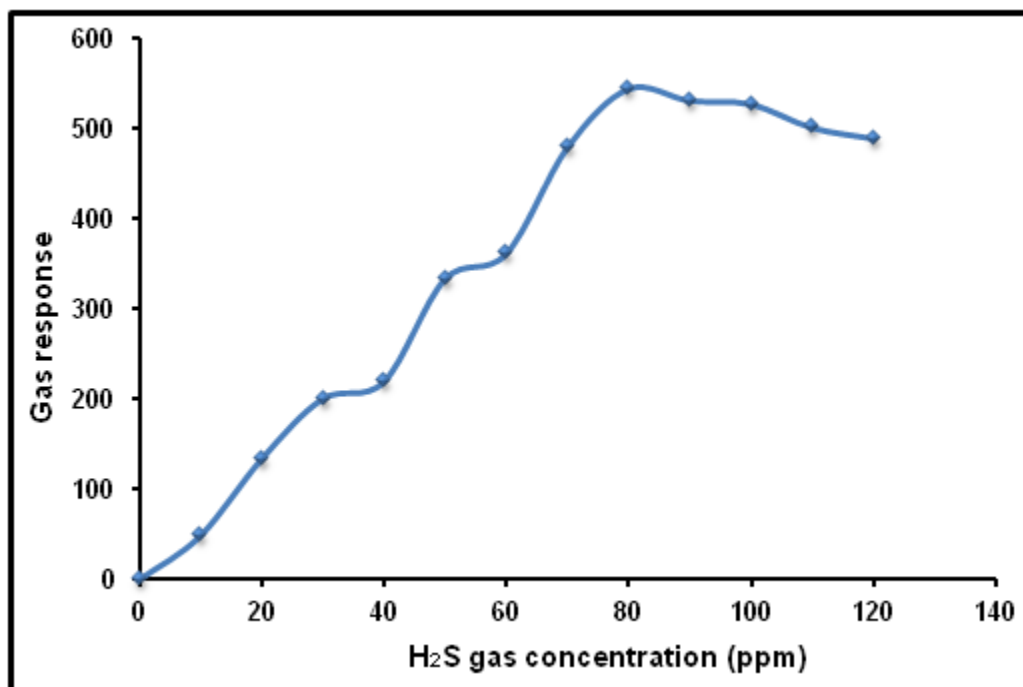

Figure 9. Variation of gas response of ST thick film with H_2S gas concentration.

iv. *Gas sensing mechanism*

Concerning the gas sensing mechanism of resistance-type semiconductor oxide materials, the sensing mechanism and change in electrical transport properties are usually involved with the adsorption and desorption process of oxygen molecules on the surface of materials [44–51]. When $SrTiO_3$ sensors are exposed to air, the oxygen molecules (O_2) of circumstance atmosphere can be adsorbed on the surface of the $SrTiO_3$ film to form adsorbed oxide ions (O_2^-, O^- or O^{2-}) via capturing electrons from the conduction band, which decreases the concentration of electrons in the conduction band and results in a higher resistance. When H_2S is introduced at the moderate temperature, the surface of $SrTiO_3$ film is exposed to the traces of the reductive gas. The interaction would occur between these adsorbed oxygen species and the reductive H_2S [50], which reduces the concentration of oxygen ions, releases free electrons to the film surface and thus increases the electron concentration (Eq. (2)), eventually increases the conductivity of the $SrTiO_3$ sensor. The reaction kinetics may be explained by the following reactions:

$$(2).$$

$$(3).$$

The presence of chemically adsorbed oxygen could cause electron depletion in the film surface and building up of Schottky surface barrier; consequently, the electrical conductance of film decreased to a minimum. The $SrTiO_3$ thick film interacts with oxygen by transferring the electron from the conduction band to adsorbed oxygen atoms. The response to H_2S can be explained as a reaction of gas with the $O_2(ads)^-$.

$$(4).$$

Actually, the theory for sensing mechanism of such sensors involves the adsorption and desorption processes, which occur at the surface of the sensing materials [46]. Therefore, the surface accessibility and high surface area are crucial to maintaining the high sensing properties of nanomaterial [49]. Thus the $SrTiO_3$ thick film sensor shows large surface accessibility, which may lead to higher sensing performance.

More gas would be adsorbed by the film surface; consequently, the gas response was enhanced. Increase in operating temperature causes oxidation of large number of H_2S molecules, thus producing very large number of electrons. Therefore, conductivity increases to a large extent. This is the reason why the gas sensitivity increases with operating temperature. However, the sensitivity decreases at higher operating temperature, as the oxygen adsorbates are desorbed from the surface of the sensor (52). Also, at higher temperature, the carrier concentration increases due to intrinsic thermal excitation and the Debye length decreases. This may be one of the reasons for decreased gas sensitivity at higher temperature (53).

VI. CONCLUSIONS

$SrTiO_3$ nanomaterial was successively synthesized using a sol-gel-hydrothermal method and its gas sensing performance was tested. The following conclusions were drawn from the present investigation:

i.   The X-ray diffraction studies of the nano powder of $SrTiO_3$ synthesized through this sol-gel-hydrothermal route have shown that the as-prepared powder was single phase, crystalline, and has a cubic perovskite structure (ABO_3) with a lattice constant $a = 3.903$ Å.

ii. The particle size calculated from FWHM is $\sim$22 nm. The phase purity of $SrTiO_3$ nanopowders has been confirmed using differential thermal analysis, thermo gravimetric analysis, and UV-visible abortion spectroscopy.

iii. The transmission electron microscopic investigation has shown that the particle size of the as-prepared powder has a mean particle size of 34 nm with standard deviation 14 nm.

iv. The band gap values obtained from the absorption spectra was found to be 3·4 eV.

v.   The maximum sensitivity was obtained at an operating temperature of 150^oC for the exposure of 80 ppm of H_2S.

vi. The results of the $SrTiO_3$ films sensing studies reveal that the as prepared material and films are a suitable for the fabrication of the H_2S gas sensor.

ACKNOWLEDGEMENTS

REFERENCES

[1] X. G. Peng, L. Manna, W. D. Yang, J. Wickham, E. Scher, A. Kadavanich, A. P. Alivisatos, "Shape control of CdSe nanocrystals", Nature, Vol. 404, No. 6773, March 2000, pp. 59-61.

[2] M. Cardona, "Optical Properties and Band Structure of $SrTiO_3$ and $BaTiO_3$", Physical Review, Vol. 140, No. 2A, 1965, pp. 651-655.

[3] C. L. Jia, K. Urban, S. Hoffmann, R. J. Waser, "Microstructure of columnar-grained SrTiO$_3$ and BaTiO$_3$ thin films prepared by chemical solution deposition" Journal of Materials Research Vol. 13, No. 08, 1998, 2206-2217.

[4] J. H. Haeni, P. Irvin, W. Chang, R. Uecker, P. Reiche, Y.L. Li, S. Choudhury, W. Tian, M.E. Hawley, B. Craigo, A.K. Tagantsev, X.Q. Pan, S.K. Streiffer, L.Q. Chen, S.W. Kirchoefer, J. Levy, D.G. Schlom, "Room-temperature ferroelectricity in strained SrTiO$_3$", Nature, Vol. 430, No. 7001, August 2004, pp. 758-761.

[5] P. Balaya, M. Ahrens, L. Kienle, J. Maier, B. Rahmati, S.B. Lee, W. Sigle, A. Pashkin, C. Kuntscher, M. Dressel, "Synthesis and Characterization of Nanocrystalline SrTiO$_3$" J. Am. Ceram. Soc. Vol. 89, No. 09, September 2006, pp. 2804-2811.

[6] Y. Hu, O.K. Tan, J.S. Pan, H. Huang, W. Cao, "The effects of annealing temperature on the sensing properties of low temperature nano-sized SrTiO$_3$ oxygen gas sensor", Sens. Actuators B, Vol. 108, No. 1-2, July 2005, pp. 244-249.

[7] T. Hara, T. Ishiguro, "Oxygen sensitivity of SrTiO$_3$ thin film prepared using atomic layer deposition", Sens. Actuators B, Vol. 136, No. 02, March 2009, pp. 489-493.

[8] S. Burnside, J.E. Moser, K. Brooks, M. Gratzel, D.J. Cahen, "Nanocrystalline Mesoporous Strontium Titanate as Photoelectrode Material for Photosensitized Solar Devices: Increasing Photovoltage through Flatband Potential Engineering", J. Phys. Chem. B, Vol. 103, No. 43 August 1999, pp. 9328-9332.

[9] L. Pellegrino, I. Pallecchi, D. Marre, E. Bellingeri, S. Siri, "Fabrication of submicron-scale SrTiO$_{3-\delta}$ devices by an atomic force microscope" Appl. Phys. Lett. Vol. 81, No. 20, November 2002, pp. 3849-3851.

[10] M.L. Moreira, J. Andres, V.M. Longo, M.S. Li, J.A. Varela, E. Longo, "Photoluminescent behavior of SrZrO$_3$/SrTiO$_3$ multilayer thin films", Chem. Phys. Lett. Vol. 473, No. 4-6, May 2009, pp. 293-298.

[11] K. Domen, A. Kudo, T. Onishi, N. Kosugi, H. Kuroda, "Photocatalytic decomposition of water into hydrogen and oxygen over nickel(II) oxide-strontium titanate (SrTiO$_3$) powder. 1. Structure of the catalysts ", J. Phys. Chem. Vol. 90, No. 02, January 1986, pp. 292-295.

[12] M.S. Wrighton, A.B. Ellis, P.T. Wolczanski, D.L. Morse, H.B. Abrahamson, D.S. Ginley, "Strontium titanate photoelectrodes. Efficient photoassisted electrolysis of water at zero applied potential", J. Am. Chem. Soc. Vol. 98, No. 10, May 1976, pp. 2774 -2779.

[13] S. Burnside, J.E. Moser, K. Brooks, M.J. Gratzel, "Nanocrystalline Mesoporous Strontium Titanate as Photoelectrode Material for Photosensitized Solar Devices: Increasing Photovoltage through Flatband Potential Engineering", Phys. Chem. B, Vol. 103, No. 43, August 1999 pp. 9328-9332.

[14] Rudiger A, Schneller T, Roelofs A, Tiedke S, Schmitz T, Waser R, "Nanosize ferroelectric oxides – tracking down the superparaelectric limit", Appl. Phys A, Vol. 80, No. 06, March 2005, pp. 1247-1255.

[15] Wu X, Wu D, Liu X, "Negative pressure effects in $SrTiO_3$ nanoparticles investigated by Raman spectroscopy", Solid State Comm., Vol. 145, No. 5-6, February 2008, pp. 255-258.

[16] H. Tagawa, K. Igarashi, "Reaction of Strontium Carbonate with Anatase and Rutile" J. Am. Ceram. Soc. Vol. 69, No. 04, April 1986, pp.310-314.

[17] V.A. Trepakov, M.E. Savinov, I. Okhay, A. Tkach, P.M. Vilarinho, A.L. Kholkin, I. Gregora, L. Jastrabik, "Dielectric permittivity and Cr^{3+} impurity ion probe luminescence in $SrTiO_3$ sol–gel ceramics", J. Eur. Ceram. Soc. Vol. 27, No. 13-15, March 2007, pp. 3705-3707.

[18] G. Pfaff, "Sol–gel synthesis of strontium titanate powders of various compositions", J. Mater. Chem. Vol.03, No. 07, July 1993, pp.721-724.

[19] Q. Pang, J.X. Shi, M.L. Gong, "Photoluminescent Properties of $SrTiO_3$: Pr, Al Nanophosphors Synthesized by Microemulsion–Microwave Heating" J. Am. Ceram. Soc. Vol. 90, No. 12, December 2007, pp. 3943- 3946.

[20] P.K. Dutta, J.R. Gregg, "Hydrothermal synthesis of tetragonal barium titanate ($BaTiO_3$)" Chem. Mater. Vol. 04, No. 04, July 1992, pp. 843-846.

[21] M.-H. Um, H. Kumazawa, "Hydrothermal synthesis of ferroelectric barium and strontium titanate extremely fine particles", J. Mater. Sci. Vol. 35, No. 05, March 2000, pp. 1295-1300.

[22] S.C. Zhang, J.X. Liu, Y.X. Han, B.C. Chen, X.G. Li, "Formation mechanisms of $SrTiO_3$ nanoparticles under hydrothermal conditions", Mater. Sci. Eng. B, Vol. 110, No. 01, June 2004 pp. 11-17.

[23] E.K. Nyutu, C.H. Chen, P.K. Dutta, S.L. Suib, "Effect of Microwave Frequency on Hydrothermal Synthesis of Nanocrystalline Tetragonal Barium Titanate" J. Phys. Chem. C, Vol. 112, No. 26, June 2008, pp. 9659-9667.

[24] E.R. Leite, C.M.G. Sousa, E. Longo, J.A. Varela, "Influence of polymerization on the synthesis of $SrTiO_3$: Part II. Particle and agglomerate morphologies", Ceram. Int., Vol. 21, No. 3, 1995, pp. 153- 158.

[25] S.M. Zanetti, E. Longo, J.A. Varela, E.R. Leite, "Microstructure and phase evolution of $SrTiO_3$ thin films on Si prepared by the use of polymeric precursors", Mater. Lett, Vol. 31, No. 3-6, June 1997, pp. 173-178.

[26] C.H. Chang, Y.H. Shen, "Synthesis and characterization of chromium doped $SrTiO_3$ photocatalyst" Mater. Lett, Vol. 60, No. 01, January 2006, pp. 129-132.

[27] H. Cui, M. Zayat, D. Levy, "Controlled homogeneity of the precursor gel in the synthesis of $SrTiO_3$ nanoparticles by an epoxide assisted sol–gel route" J. Non-Cryst. Solids, Vol. 353, No. 11-12, May 2007, pp. 1011-1016.

[28] Yoshimura M, "Importance of soft solution processing for advanced inorganic materials", J Mater Res, Vol.- 13, No. 04,: April1998, pp.796-802.

[29] J. Kong, N. Franklin, C. Zhou, M. Chapline, S. Peng, K. Cho, H. Dai, Nanotube molecular wires as chemical sensors, Science Vol. 287, January 2000, pp. 622–625.

[30] W. Gopel, K. Schierbaum, SnO_2 sensors current status and future prospects, Sens. Actuators B, Vol. 26, No. 1-3, June 1995, pp. 1–12.

[31] Y. Yamada, Y. Seno, Y. Masuoka, K. Yamashita, Nitrogen oxides sensing characteristics of Zn_2SnO_4 thin film, Sens. Actuators B, Vol. 49, No.3, July 1998, pp. 248–252.

[32] G. Korotcenkov, Gas response control through structural and chemical modification of metal oxide films: state of the art and approaches, Sens. Actuators B, Vol. 107, No. 01, May 2005, pp. 209–232.

[33] G. Otulakowski, B.P. Kavanagh, Hydrogen sulfide in lung injury: therapeutic hope from a toxic gas? Anesthesiology, Vol. 113, No. 1, July 2010, pp. 4–6.

[34] D. Vuong, G. Sakai, K. Shimanoe, N. Yamazoe, Hydrogen sulfide gas sensing properties of thin films derived from SnO_2 sols different in grain size, Sens. Actuators B, Vol. 105, No. 2, March 2005, pp. 437–442.

[35] I. S. Hwang, J.K. Choi, S.J. Kim, K.Y. Dong, J.H. Kwon, B.K. Ju, J.H. Lee, Enhanced H_2S sensing characteristics of SnO_2 nanowires functionalized with CuO, Sens. Actuators B, Vol. 142, No. 01, October 2009, pp. 105-110.

[36] J. Xu, X. Wang, J. Shen, Hydrothermal synthesis of In_2O_3 for detecting H_2S in air, Sens. Actuators B, Vol. 115, No. 02, June 2006, pp. 642–646.

[37] G. H. Jain, V. B. Gaikwad and L. A. Patil, "Studies on gas sensing performance of $(Ba_{0.8}Sr_{0.2})(Sn_{0.8}Ti_{0.2})O_3$ thick film resistors", Sensors and Actuators B, Vol. 122, No. 02, March 2007, pp. 605-612.

[38] G. H. Jain, V. B. Gaikwad, D. D. Kajale, R. M. Chaudhari, R. L. Patil, N. K. Pawar and L. A. Patil, "Gas Sensing Performance of pure and modified Barium Strontium Titanate Thick Film Resistors", Sensors and Transducers, Vol. 90, 2008, pp. 160-173

[39] P. Balaya, J. Jamnik, J. Fleig, J. Maier, "Mesoscopic electrical conduction in nanocrystalline $SrTiO_3$"Appl. Phys. Lett. Vol. 88, No. 6, February 2006, article no. 062109 (3 pages).

[40] F.M. Pontes, E. Longo, E.R. Leite, E.J.H. Lee, J.A. Varela, P.S. Pizani, "Photoluminescence at room temperature in amorphous $SrTiO_3$ thin films obtained by chemical solution deposition", Mater. Chem. Phys. Vol. 77, No. 02, January 2002, pp. 598–602.

[41] C.D. Pinheiro, E. Longo, E.R. Leite, F.M. Pontes, R.Magnani, J.A. Varela, The role of defect states in the creation of photoluminescence in $SrTiO_3$, Appl. Phys. A, Vol. 77, No. 1, 2003, pp. 81–85.

[42] W.F. Zhang, Z. Yin, M.S. Zhang, Study of photoluminescence and electronic states in nanophase strontium titanate, Appl. Phys. A, Vol. 70, No. 01, 2000, pp. 93–96.

[43] Y.S. Kim, S.C. Ha, K. Kim, H. Yang, J.T. Park, C.H. Lee, J. Choi, J. Paek, K. Lee, Room temperature semiconductor gas sensor based on non-stoichiometric tungsten oxide nanorod film, Appl. Phys. Lett. Vol. 86, No. 21, May 2005, article no. 213105(3pages).

[44] N. Yamazoe, New approaches for improving semiconductor gas sensors, Sens. Actuators B, Vol. 5, 1991, pp.7–19.

[45] Z. Gergintschew, H. Förster, J. Kositza, D. Schipanski, Two-dimensional numerical simulation of semiconductor gas sensors, Sens. Actuators B, Vol. 26, 1995, pp.170–173.

[46] N. Yamazoe, G. Sakai, K. Shimanoe, Oxide semiconductor gas sensors, Catal. Surv. Asia Vol. 7 2003, pp. 63–75.

[47] T. Gao, T.H. Wang, Synthesis and properties of multipod-shaped ZnO nanorods for gas sensor applications, Appl. Phys. A, Vol. 80, 2005, pp.1451–1454.

[48] N. Yamazoe, J. Fuchigami, M. Kishikawa, T. Seiyama, Interactions of tin oxide surface with O_2, H_2O and H_2, Surf. Sci., Vol. 86, 1979, pp. 335–344.

[49] M. Egashira, Y. Shimizu, Y. Takao, S. Sako, Variations in I–V characteristics of oxide semiconductors induced by oxidizing gases , Sens. Actuators B, Vol.35, 1996, pp.62–67.

[50] J.Q. Xu, X.H. Jia, X.D. Lou, J.N. Shen, One-step hydrothermal synthesis and gas sensing property of $ZnSnO_3$ microparticles , Solid State Electron. Vol. 50, No. 3, 2006, pp. 504–507.

[51] A. Rothschild and Y. Komen, "The effect of grain size on the sensitivity of nanocrystalline metal-oxide gas sensors" J. Appl. Phys. Vol. 95, No. 11, 2004, pp. 6374-6380.

[52] H. Windichamann and P. Mark, "A Model for the Operation of a Thin-Film SnO_x Conductance-Modulation Carbon Monoxide Sensor", J. Electrochem. Soc. Vol. 126, No. 4, 1979, pp.627-633.

[53] J Mizsei, How can sensitive and selective semiconductor gas sensors be made? Sensors and Actuators B, Vol. 23, No. 2- 3, February 1995, pp. 173-176